

Measurement of Lower-Hybrid Drift Turbulence in a Reconnecting Current Sheet

T. A. Carter,* H. Ji, F. Trintchouk, M. Yamada, and R. M. Kulsrud

Princeton University, Plasma Physics Laboratory, P.O. Box 451, Princeton, New Jersey 08543

(Received 13 June 2001; published 19 December 2001)

We present a detailed study of fluctuations in a laboratory current sheet undergoing magnetic reconnection. The measurements reveal the presence of lower-hybrid-frequency-range fluctuations on the edge of current sheets produced in the magnetic reconnection experiment (MRX). The measured fluctuation characteristics are consistent with theoretical predictions for the lower-hybrid drift instability (LHDI). Our observations suggest that the LHDI turbulence alone cannot explain the observed fast reconnection rate in MRX.

DOI: 10.1103/PhysRevLett.88.015001

PACS numbers: 52.35.Vd, 52.35.Qz, 52.35.Ra, 52.72.+v

Magnetic reconnection [1] is an important process in magnetized plasmas in which a rapid release of magnetic energy and changes in magnetic topology can occur even in highly conducting plasma. Recent simulations [2] and experiments [3] have shown that current sheets associated with reconnection have widths on the order of the ion skin depth ($c/\omega_{p,i}$), a scale on which the magnetohydrodynamic (MHD) model is likely to be inaccurate. There are two theoretical models in the literature which address the problem of fast reconnection in non-MHD current sheets. The first invokes microinstability-produced anomalous resistivity [4] which enhances the rate of magnetic field dissipation and broadens the current layer to assist in the outflow of mass. The second theoretical model invokes nondissipative terms in the generalized Ohm's law, specifically the Hall term, which can lead to laminar fast reconnection in collisionless plasmas [5]. Experimental data on the nature and role of turbulence in reconnecting current sheets is needed to resolve the obvious controversy presented by these two theoretical perspectives. Motivated by this goal, we have carried out a detailed experimental study of fluctuations which has led to the first observation of the lower-hybrid drift instability in a laboratory current sheet.

The lower-hybrid drift instability (LHDI) [6] is driven by cross-field currents and density gradients present in current sheets. It has a real frequency near the lower-hybrid frequency ($\omega_{LH} \sim \sqrt{\Omega_e \Omega_i}$) and inverse wave number near the electron gyroradius ($k\rho_e \sim 1$). The LHDI has been proposed as a source of anomalous resistivity in reconnecting current sheets [7]. However, theoretical studies of the LHDI have revealed that the instability is linearly stabilized by large plasma beta [6], which should confine the instability to the edges of a current sheet. Three-dimensional particle simulations [8] and Hall MHD simulations [9] have actually shown that the LHDI does develop in the current sheet, but have conflicting views on the role of the turbulence: The former shows that LHDI can assist in driving reconnection (through profile modification or by assisting in electric field penetration), while the latter shows that LHDI is not important and may actually slow reconnection relative to

laminar two-dimensional simulations. While there is some observational evidence for the existence of the LHDI in the magnetotail current sheet [10], it has never before been detected in a laboratory current sheet. Earlier laboratory studies of fluctuations have revealed evidence for unstable ion acoustic and whistler waves in current sheets [11], but the ion gyroradius in these experiments was larger than the apparatus size, and excitation of instabilities such as the LHDI might not have been possible.

The experiments reported here were performed in the magnetic reconnection experiment (MRX) [12]. In MRX well diagnosed, long lived current sheets ($\tau \gg \tau_A$) are formed in plasmas in which MHD is satisfied in the bulk of the plasma [S (Lundquist number) $\gg 1$ and $\rho_i \ll L$ away from the current sheet]. A schematic of the MRX device is shown in Fig. 1, along with a single magnetic field line indicating the current sheet location. Collisionality in MRX current sheets is characterized by the parameter λ_{mfp}/δ , where δ is the width of the current sheet, and λ_{mfp} is the electron mean free path. Two observations have been made as the collisionality was lowered (λ_{mfp}/δ is increased) in MRX. The first is that the measured toroidal reconnection electric field, E_θ , is no longer balanced by classical collisional drag at the center of the current sheet, $E_\theta/\eta_{sp}j_\theta \gg 1$, where η_{sp} is the classical Spitzer perpendicular resistivity [13]. The second is that direct, nonclassical ion heating has been observed during reconnection in MRX and the heating was found to strengthen with lower collisionality [14]. One possible explanation for these observations is the presence of turbulence in low-collisionality MRX current sheets, which creates a turbulent anomalous resistivity $\eta^* > \eta_{sp}$ (so that $E_\theta/\eta^*j_\theta = 1$) and directly heats the ions. Detailed high-frequency fluctuation measurements were made in MRX in order to test this hypothesis. Two types of diagnostics were used for this study: floating double Langmuir probes with 0.1 to 0.7 mm diameter tungsten tips, and magnetic pickup loops (3 mm diameter, 80 turns). In both types of probes, miniature buffer amplifiers were embedded near the probe tips for improved immunity from discharge circuit noise and for ease of impedance matching. The probes used in

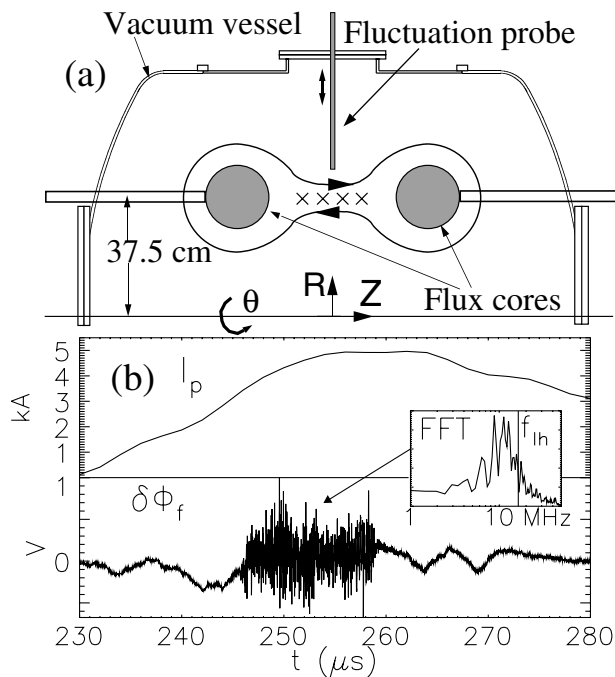


FIG. 1. (a) Schematic of the MRX apparatus with fluctuation probe. Current sheet location is denoted by \times 's. (b) Traces of plasma current and measured floating potential signal along with an FFT of the signal. Current sheet formation and reconnection occur roughly from $t = 240$ to $280 \mu\text{s}$.

these studies were inserted into the MRX current sheet radially, as shown in Fig. 1(a). Radial profiles were obtained through shot-to-shot positioning of the probes and through averaging over several shots at each position. The experiments reported here were performed in current sheets where no toroidal guide field was imposed.

Typical time traces of the total plasma current and measured signal from a floating double Langmuir probe located at the edge of the MRX current sheet are shown in Fig. 1(b). High-frequency signals are seen to arise with the formation of the current sheet and persist for tens of microseconds. The amplitude of the measured fluctuations is found to be several percent of the electron temperature ($e\phi/kT_e \sim 5\% - 10\%$). A fast Fourier transform (FFT) of this example signal shows a rather broad power spectrum located near the lower-hybrid frequency ($f_{LH} \sim 16 \text{ MHz}$, computed from the locally measured magnetic field). High-frequency magnetic field fluctuations are also observed concomitantly in space and time with the floating potential signals, with very similar frequency spectrum. The amplitude of the measured magnetic fluctuations is on the order of $5 - 10 \text{ G}$ ($\delta B/B_0$ a few percent) and is strongest in the reconnecting field component (B_z).

The detailed dependence of the frequency spectrum of the fluctuations on the local lower-hybrid frequency was explored through varying the capacitor bank voltage (which changes the peak field in the current sheet) and the mass of the working gas. Figure 2 shows the frequency

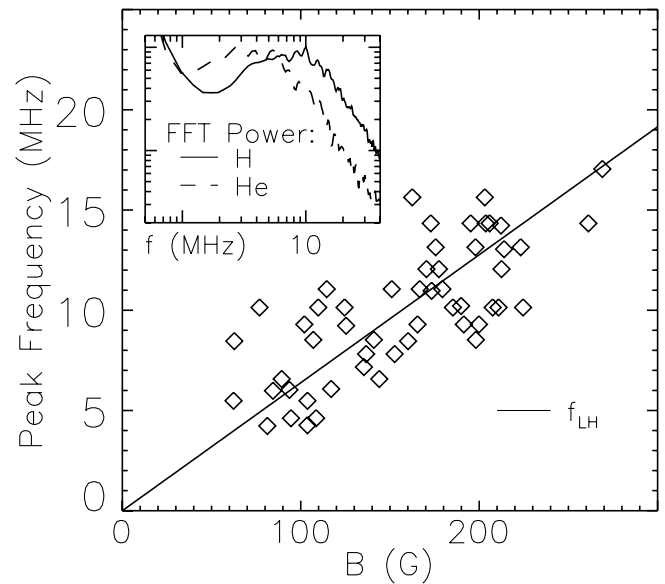


FIG. 2. Frequency at peak fluctuation amplitude versus locally measured magnetic field value, along with the lower hybrid frequency (f_{LH}), for discharges in hydrogen. Inset: Log-log plot of average fluctuation spectra in hydrogen and helium discharges.

of peak fluctuation amplitude versus local magnetic field value for discharges in hydrogen. The peak frequency increases with increasing local magnetic field and compares well with the lower-hybrid frequency, which is plotted for reference. An additional plot is inset in Fig. 2 showing plots of the average FFT power in the fluctuations in hydrogen and helium discharges with similar values of local B . A clear down-shift in the frequency spectrum is observed with increasing mass, consistent with the factor of 2 decrease in the lower-hybrid frequency. These observed scalings in the spectrum with B and ion mass are consistent with expectations for the LHDI.

Figure 3(a) shows average radial profiles of the fluctuating floating potential amplitude superimposed on the deduced average current density profile at four times during a set of more than 200 low-collisionality ($\lambda_{mf}/\delta \sim 5 - 10$) MRX discharges. The magnetic field profile in MRX is well described by the Harris sheet equilibrium model [3], and the current profiles shown in this figure are computed through fitting the average magnetic field measurements to the Harris profile and then deriving the current density from the fit. The fluctuation amplitude is concentrated on the inner edge of the current sheet and is observed to grow as the current sheet forms and reconnection begins, but then decay even while reconnection persists. In order to explain the spatial profiles and temporal behavior of the measured instability amplitude, linear calculations of the local growth rate of the LHDI in the MRX current sheet were performed. An electrostatic local theory was employed which includes finite plasma beta effects through ∇B drift corrections to the electron orbits. The following expression is found for the dispersion of the LHDI in this limit [6,15]:

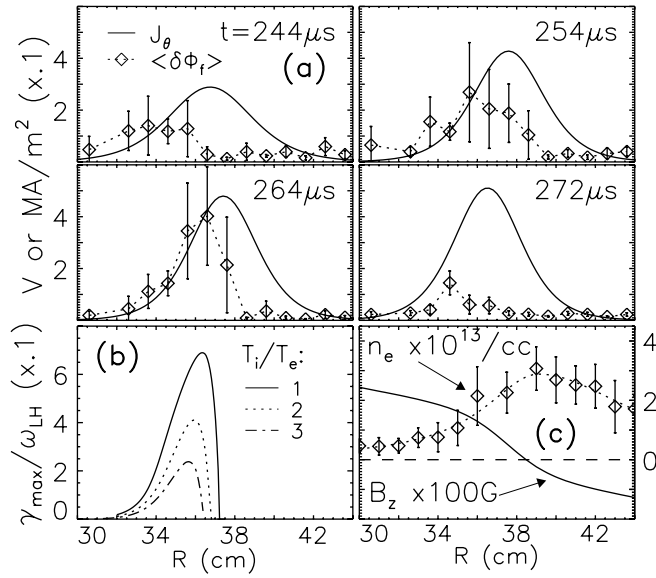


FIG. 3. (a) Average radial profile of root mean square floating potential fluctuation amplitude at four time points. (b) Maximum LHDH linear growth rate profile computed using measured plasma parameter profiles at $t = 264 \mu s$. (c) Profiles of n_e and B_z showing asymmetries which explain the asymmetric fluctuation amplitude profile.

$$0 = 1 - \frac{\omega_{p,i}^2}{2k^2 v_{th,i}^2} Z' \left(\frac{\omega - \mathbf{k} \cdot \mathbf{V}}{k v_{th,i}} \right) + \frac{\omega_{p,e}^2}{k^2 v_{th,e}^2} [1 + \psi], \quad (1)$$

$$\psi = 2 \frac{\omega}{k_{\parallel} v_{th,e}} \left(1 - \frac{k_y V_{d,e}}{\omega} \right) \times \int_0^{\infty} dx x \exp(-x^2) J_0^2(k_{\perp} \rho_e x) Z \left(\frac{\omega - k_y V_B x^2}{k_{\parallel} v_{th,e}} \right),$$

where $Z(x)$ is the plasma dispersion function, $\omega_{pe/i}$ is the electron/ion plasma frequency, $V_{d,e}$ is the electron diamagnetic drift speed, $V_B = \beta V_{d,e}/2$ is the electron ∇B drift velocity, $x = v_{\perp}/v_{th,e}$, and V is the cross-field ion drift. Using measured profiles of B_z , n_e , and T_e at $t = 264 \mu s$, the profile of the maximum LHDH growth rate was computed using Eq. (1) (assuming $T_i/T_e = 1, 2, 3$) and is shown in Fig. 3(b). The computed maximum growth rate profile is asymmetric with respect to the current sheet and compares well with the fluctuation amplitude profile at $t = 264 \mu s$. The asymmetry in the predicted growth rate comes from asymmetries in the measured density gradient (which drives the instability) and the magnetic field profile across the current sheet at $t = 264 \mu s$, as shown in Fig. 3(c). These two asymmetries, which are consistent with radial force balance [3], combine to produce a strong asymmetry in the plasma beta across the current sheet, with a larger, stabilizing beta on the outer edge. It should be noted that the fluctuation amplitude is insignificant at the magnetic null, which is offset from the current density peak due to toroidal effects [evident when comparing Fig. 3(c) to the current and fluctuation amplitude profile in Fig. 3(a) at $t = 264 \mu s$].

The observed decrease in the fluctuation amplitude after $t = 264 \mu s$ could be due to ion heating during reconnection, since the linear growth rate of the LHDH decreases with increasing T_i/T_e [see Fig. 3(b)]. Spectroscopic ion temperature measurements in helium discharges in MRX have shown significant ion heating to temperature ratios of $T_i/T_e \geq 1$ during reconnection [14]. In hydrogen, direct ion temperature measurements have not been performed; however, estimates of T_i based on radial force balance yield temperature ratios of $T_i/T_e \geq 2$ during the reconnection process.

Spatial correlations in the LHDH turbulence were also studied, using spatially separated probes. Measurements were performed using probe spacings of 1, 3.5, and 10 mm ($\rho_e \sim 0.5$ mm) in the toroidal direction. The mean coherency between separated probe signals (ϕ_1, ϕ_2) was calculated for signals from probes at these separations through averaging the coherency $[\gamma = |\phi_1 \phi_2^*| / (|\phi_1| |\phi_2|)]$ over the measured LHDH spectrum and over 20 similar discharges per separation. Figure 4(a) shows the mean coherency for each of the three different probe separations. The average decorrelation length in the turbulence can be estimated from this data to be several ρ_e , which is comparable to the wavelength at peak growth for the LHDH ($\lambda \sim 2\pi\rho_e$). This observation is consistent with the predicted strong linear growth rate ($\gamma \sim \omega_r$) for the LHDH in MRX. Attempts to quantitatively measure the phase velocity of the waves were hindered likely due to the observed short decorrelation length, although a hint of preference for propagation in the electron diamagnetic direction is observed.

The final point to address in this Letter is the role of the measured turbulence in the process of magnetic reconnection in MRX. Two observations shown in Fig. 3 cast doubt on the possibility of the LHDH playing a direct role in determining the reconnection rate in MRX. The first observation is that the measured amplitude profile is consistent with finite-beta stabilization of the LHDH, showing that the instability is restricted to regions of low beta, away from the magnetic null where it would be needed to

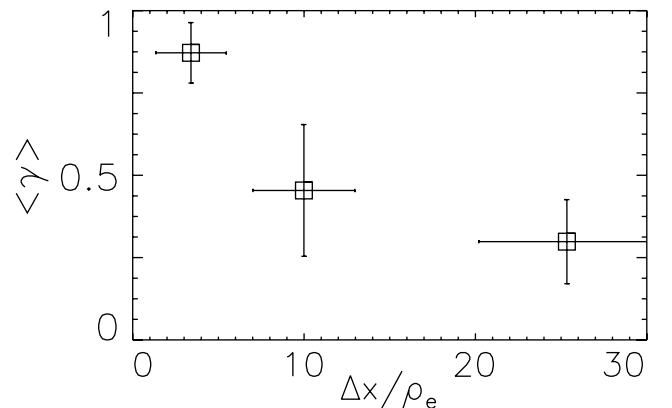


FIG. 4. Mean coherency in spatially separated floating potential signals (separations: 1, 3.5, and 10 mm).

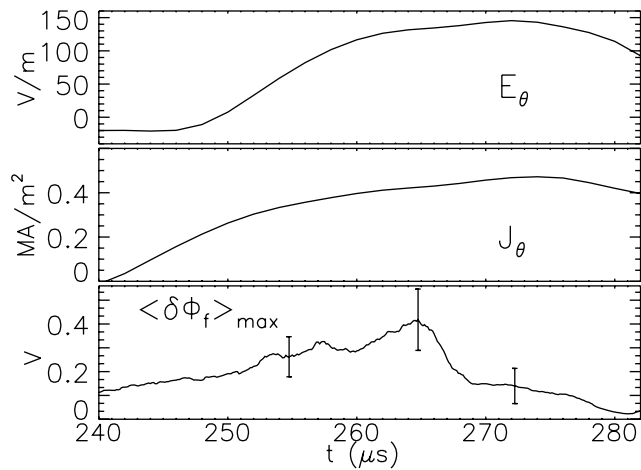


FIG. 5. Time history of toroidal electric field at the null line, peak current density, and peak fluctuation amplitude.

generate enough anomalous resistivity to balance the electric field in the resistive MHD Ohm's law. The second observation is the rapid decay of the fluctuation amplitude early in the reconnection process. Figure 5 makes this observation clearer by comparing the time behavior of the reconnection electric field (which is directly related to the reconnection rate), the peak current density, and the peak fluctuation amplitude. The fluctuation amplitude is observed to decay rapidly during reconnection while the reconnection electric field and current density remain steady (or might even *increase* slightly). If the LHDI was directly responsible for the observed fast reconnection rate in MRX it would be reasonable to expect a correlation between the instability amplitude and the rate of reconnection; this correlation does not seem to exist in the data shown here. An additional set of data was taken to explore the dependence of the fluctuation amplitude on the collisionality in MRX current sheets. It was previously found that the measured resistivity enhancement, $E_\theta/\eta_{sp}j_\theta$, increased dramatically as the collisionality was lowered in MRX [13]. If the LHDI was responsible for this increase, a similar trend in the fluctuation amplitude might be expected. Figure 6(a) shows the measured peak fluctuation amplitude (peak amplitude in both space and time) versus λ_{mfp}/δ from a scan of fill

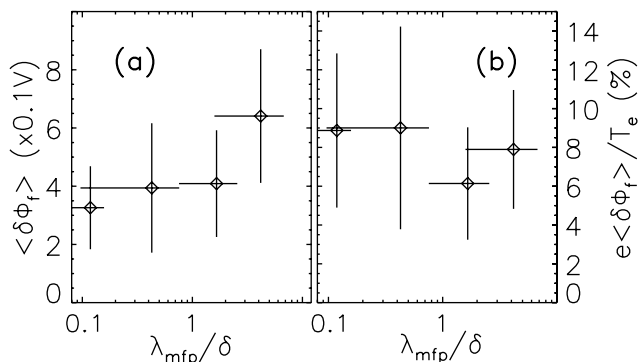


FIG. 6. (a) Fluctuation amplitude and (b) normalized fluctuation amplitude versus collisionality from a scan in fill pressure.

pressure. The amplitude of the fluctuations does increase slightly with decreasing collisionality (increasing λ_{mfp}/δ). However, if the fluctuation amplitude is normalized to the measured electron temperature, which might be considered an estimate of $\delta n/n$ in the turbulence and therefore proportional to the effective collisionality, we find that there is essentially no change in this quantity with collisionality, as shown in Fig. 6(b).

In conclusion, we have made detailed measurements of fluctuations in MRX, resulting in the first observation of the lower-hybrid drift instability in a laboratory current sheet. This observation has allowed the unprecedented opportunity to experimentally investigate the role of this instability in magnetic reconnection. The measurements described here suggest that the LHDI is not essential in determining the reconnection rate in MRX current sheets. Although the measurements reported in this Letter make it difficult to explain reconnection in MRX through simply extending MHD theories with a turbulent anomalous resistivity, they do not directly support alternative theories such as those based on the Hall term. Future experiments in MRX will search for signatures of the Hall theories while continuing to investigate the role of turbulence in the current sheet. The results reported here may also be relevant to reconnection in space plasmas, such as in the magnetotail, where evidence for the presence of the LHDI exists.

The authors thank D. Cylinder and R. Cutler for their excellent technical assistance and S. Hsu for useful discussions. T.A.C. acknowledges support from NSF and NASA. MRX is jointly funded by DOE, NASA, and NSF.

*Present address: Department of Physics and Astronomy, University of California, Los Angeles, CA 90095-1547.

Electronic address: tcarter@physics.ucla.edu

- [1] D. Biskamp, Phys. Rep. **237**, 179 (1994).
- [2] D. Biskamp, E. Schwarz, and J. F. Drake, Phys. Rev. Lett. **75**, 3850 (1995).
- [3] M. Yamada *et al.*, Phys. Plasmas **7**, 1781 (2000).
- [4] J. Heyvaerts, E. Priest, and D. Rust, Astrophys. J. **216**, 123 (1977).
- [5] J. Birn *et al.*, J. Geophys. Res. Space Phys. **106**, 3715 (2001).
- [6] R. Davidson, N. Gladd, C. Wu, and J. Huba, Phys. Fluids **20**, 301 (1977).
- [7] J. Huba, N. Gladd, and K. Papadopoulos, Geophys. Res. Lett. **4**, 125 (1977).
- [8] R. Horiuchi and T. Sato, Phys. Plasmas **6**, 4565 (1999).
- [9] B. Rogers, J. Drake, and M. Shay, Geophys. Res. Lett. **27**, 3157 (2000).
- [10] I. Shinohara *et al.*, J. Geophys. Res. **103**, 20365 (1998).
- [11] W. Gekelman and R. Stenzel, J. Geophys. Res. **89**, 2715 (1984).
- [12] M. Yamada *et al.*, Phys. Plasmas **4**, 1936 (1997).
- [13] H. Ji, M. Yamada, S. Hsu, and R. Kulsrud, Phys. Rev. Lett. **80**, 3256 (1998).
- [14] S. Hsu *et al.*, Phys. Plasmas **8**, 1916 (2001).
- [15] J. Huba and C. Wu, Phys. Fluids **19**, 988 (1976).